

# The description of spatial pattern using two-dimensional spectral analysis

E. Renshaw[1] & E. D. Ford[2]
[1] *Department of Statistics, University of Edinburgh, King's Buildings, Mayfield Road, Edinburgh EH9 3JZ, United Kingdom*
[2] *Institute of Terrestrial Ecology, Bush Estate, Penicuik, Midlothian EH26 0QB, United Kingdom*

Keywords: Inhibition, Invasion, Pattern, Simulation, Spectral analysis, Vegetation analysis

## Abstract

Two-dimensional spectral analysis is a general interrogative technique for describing spatial patterns. Not only is it able to detect all possible scales of pattern which can be present in the data but it is also sensitive to directional components.

Four functions are described: the autocorrelation function; the periodogram; and, the $R$- and $\Theta$-spectra which respectively summarize the periodogram in terms of scale and directional components of pattern. The use of these functions is illustrated by their application to a simple wave pattern, a wave pattern with added noise, and patterns simulating competition and invasion processes.

## Introduction

Watt (1947) advanced the thesis that by studying how the pattern of plants in a community changed with time deductions could be made as to the important processes controlling ecosystem development. Greig-Smith (1952) recognized that these descriptions of pattern should be quantified, and proposed the technique whereby plant frequency is counted in an array of contiguous quadrats and a nested analysis of variance calculated with the quadrats considered in ordered groupings of increasing size. This technique has been used extensively to describe different scales of pattern in vegetation (see Greig-Smith (1979) for a review).

However, the generality of Greig-Smith's technique is limited in two important respects which can affect its value in an exploratory examination of pattern. First, scales of pattern can only be detected at the size of the individual quadrat and at multiplications of 2, 4, 8, ... of this size, and so some pattern may be missed. Moreover, where the quadrat size is close to the smallest scale of pattern then the precise starting point of the sample within the pattern will influence the degree to which this scale is detected. Second, the technique will not detect directional components of a pattern, i.e. anisotropy. This is an important limitation, because plants may be subject to directional biological or environmental stimuli.

Two-dimensional spectral analysis overcomes both of these problems. For the variance of the data is split into far more general components than the powers of two, each component being a measure of the contribution of a specific frequency of occurrence of a particular pattern. This technique is analogous to turning the tuning knob on a radio, identification of a scale of pattern being akin to identifying the wavelength of a radio signal. Indeed, two-dimensional spectral analysis provides a comprehensive description of both the structures and scales of pattern in a spatial data set and so is a general interrogative technique.

Spectral analysis of line transects of contiguous quadrats, i.e. samples in *one dimension,* has been compared with other techniques for the analysis of pattern. Ripley (1978) concluded 'Spectral analysis is by a wide margin the most reliable and informa-

Vegetatio 56, 75–85 (1984).

tive method', though he added that experience is needed to avoid misinterpretation of spectra. Hill (1973) commented that spectral analysis is the technique most sensitive to regularities in the data which make it the most likely to pick up both real patterns and 'spurious' effects, whilst Usher (1975) concluded that, 'Spectral analysis appears to be sufficiently robust for the analysis of data with a large stochastic element, however the main problem is spurious peaks in the analysis owing to the discrete nature of the majority of botanical data'. Thus the sensitivity of spectral analysis and its ability to reveal the range of patterns in a data set is acknowledged but the objective assessment of the analysis is questioned.

Here we describe two-dimensional spectral analysis through analysis of data containing some simple patterns. Subsequently (Ford & Renshaw, 1984) we describe how the analysis of field data, in combination with that of simulated patterns, can be used to build models of pattern generating processes in vegetation. Programs to compute all the analyses described here may be obtained directly from the authors, and so it is not necessary to have a full appreciation of the mathematical details involved in the calculations.

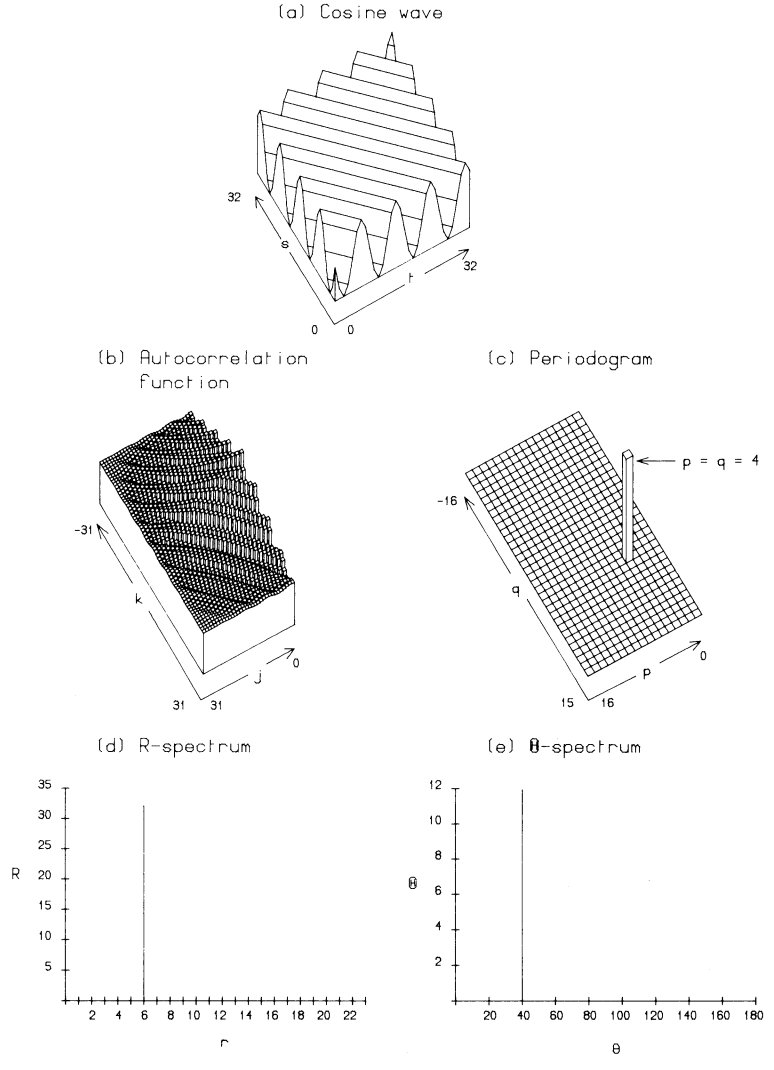


*Fig. 1.* Spatial analysis of a pure cosine wave with $p = q = 4$. (a) cosine wave; (b) autocorrelation function; (c) periodogram; (d) $R$-spectrum; (e) $\Theta$-spectrum.

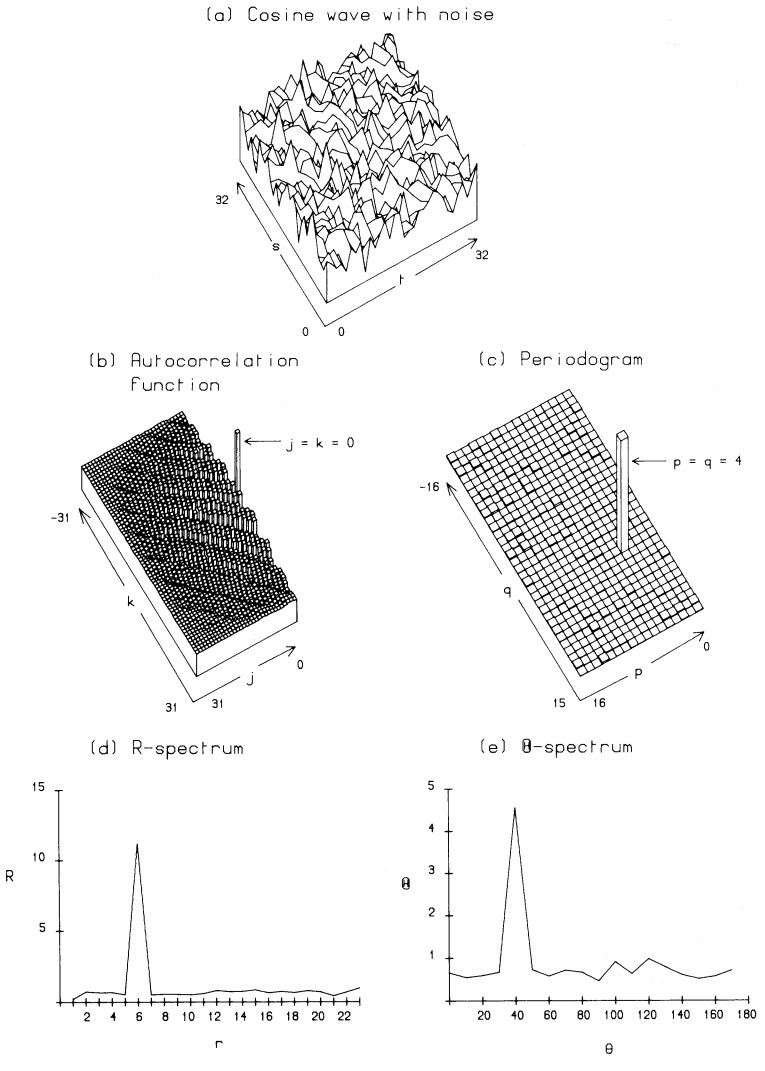


*Fig. 2.* Spatial analysis of a pure cosine wave (Fig. 1a) with added random noise, see text. (a) cosine wave with noise; (b) autocorrelation function; (c) periodogram; (d) *R*-spectrum; (e) Θ-spectrum.

## Two-dimensional spectral analysis

Two-dimensional spectral analysis does not describe pattern by a single statistic; four main functions are used which we illustrate by their application to two patterns of known structure. The first pattern is a cosine wave at 45° to a Cartesian sampling frame and with four complete cycles along each axis (Fig. 1a) generated by calculating $\cos[2\pi\{(ps/m)+(qt/n)\}]$ where $m = n = 32$, i.e. the number of points per axis, and $p = q = 4$. For the second pattern we calculated a cosine wave in the same way, but to each of the individual $32 \times 32$ elements random noise was added from a Normal distribution with mean 0 and standard deviation 1. In this resulting pattern (Fig. 2a) the underlying cosine wave is not discernible. Analysis is made after subtracting the mean of the $32 \times 32$ array from each element, and we denote this mean-corrected array by $X_{st}$ ($s = 1, \ldots, m$; $t = 1, \ldots, n$).

Complete output of the periodogram, polar-spectrum and autocorrelations described below may be obtained with the authors' program from a single command. Two versions are available: a

computationally slow program requires only that the number of rows ($m$) and columns ($n$) are even; a far faster program requires $m$ and $n$ to be powers of 2. For $m \times n$ in excess of $50 \times 50$ the fast version is recommended if cpu time is important, but this requires $m$ and $n = 64, 128, 256$, etc. However, the danger of non-stationarity, i.e. a trend in pattern across the plot, may increase with $m$ and $n$, and a $50 \times 50$ data set is usually more than sufficient to detect all scales of pattern of interest provided the sampling intensity is sensibly chosen. We have often used $32 \times 32$, and even $20 \times 20$, successfully. For large data sets sub-division into non-overlapping rectangles enables consistency of pattern to be checked.

*Sample autocovariance*

We define the *sample autocovariance* at lag $(j, k)$ for $0 \leqslant j < m$ and $-n < k < n$ by

$$C_{jk} = (1/mn) \sum_{s=1}^{m-j} \sum_{t} X_{st} X_{s+j,\, t+k} \qquad (1)$$

where the second summation is taken over $t = 1, \ldots, n\text{-}k$ if $k \geqslant 0$ and over $t = -k+1, \ldots, n$ if $k < 0$. The *spatial autocorrelation matrix* is then given by $\{C_{jk}/s^2\}$ where $s^2$ denotes the sample variance of the $\{X_{st}\}$. The full spatial autocorrelation matrix has a central value of $C_{oo}/s^2 = 1$, i.e. the data 'correlates perfectly' with itself, and the values at increasing distances from the center are estimates of the correlation between points and their successively more distant neighbours. Conventionally, and as expressed in (1), each possible neighbour pair is represented only once, and a matrix of entries almost twice the size of the data matrix is obtained (Fig. 1b). The sample autocovariance of a cosine wave is itself a cosine wave, but with the individual entries having decreasing amplitude with increasing distance from the central point, as at increasing lags $(j, k)$ fewer products are summed in the calculation of the individual entries in the function (1) though the denominator ($mn$) remains constant. There is positive correlation between neighbours in the direction along the waves, whether the points themselves are on a ridge or in a trough, and moving across the waves first negative correlation and then positive correlation as the displacement (lag) advances to the degree where the pattern repeats itself which here is at $(j, k) = (32/4, 32/4)$, i.e. (8,8). The autocovariance function of the pattern with noise added (Fig. 2b) has a similar structure to Figure 1b except that the individual entries are of smaller amplitude save, of course, for $C_{jk}/s^2 = 1$ at $j = k = 0$. Thus the addition of noise, which is always present in real data, reduces the size and clarity of the autocorrelation structure but not the overall effect.

*The periodogram*

A more compact description of spatial pattern is often obtained by evaluating the *periodogram* or *sample spectral function;* this shows the extent to which the data contains periodicities at different frequencies. The data is transformed by cosine waves of different wavelengths which, in the analogy of tuning a radio set, represent discrete but small bands of reception. The transformation apportions the sample variance between the range of frequencies. The size of the sample area limits the detection of low frequency, i.e. large-scale patterns, whilst the number of sample units $(m, n)$ limits the detection of high frequency, i.e. small-scale patterns.

The periodogram may be calculated via either the autocovariance function

$$I_{pq} = \sum_{j=-m+1}^{m-1} \sum_{k=-n+1}^{n-1} C_{jk} \cos\{2\pi(\frac{jp}{m} + \frac{kq}{n})\} \qquad (2)$$

or, equivalently, directly through

$$I_{pq} = mn(a_{pq}^2 + b_{pq}^2) \qquad (3)$$

where

$$a_{pq} = (1/mn) \sum_{s=1}^{m} \sum_{t=1}^{n} X_{st} \cos[2\pi(\frac{ps}{m} + \frac{qt}{n})] \qquad (4)$$

and

$$b_{pq} = (1/mn) \sum_{s=1}^{m} \sum_{t=1}^{n} X_{st} \sin[2\pi(\frac{ps}{m} + \frac{qt}{n})] \qquad (5)$$

The full range of frequencies is over $p = 0, \ldots, m\text{-}1$; $q = 0, \ldots, n\text{-}1$, but because of the symmetry relation $I_{m-p,q} = I_{p,n-q}$ we need only consider the half-periodogram $p = 0, \ldots, m/2$; $q = -n/2, \ldots, n/2\text{-}1$ (for $m$ and $n$ even). This choice of $p,q$-values is appropriate, for the sign of $q$ relates to the direction of

travel of the waves: $q$ positive or negative implies a general NW-SE or NE-SW alignment, respectively.

The periodogram (Fig. 1c) of the cosine wave pattern has a single entry at $p = q = 4$, i.e. $I_{44}$, which accounts for all the variance. This shows the pattern is a wave which repeats 4 times in 32 units along both axes; i.e. the waves are aligned at 90° to the diagonal line joining the coordinates (1,1) and (32,32), and the wavelength along that line is $(32\sqrt{2})/8 = 4\sqrt{2}$. The simplicity of Figure 1c compared to Figure 1b illustrates the effectiveness of the periodogram relative to the autocovariance function.

Although the addition of noise to the cosine wave reduces the contribution of the single periodogram value $I_{44}$ to total variance from 100% to 33.14%, $I_{44}$ still totally dominates the periodogram (Fig. 2c). Formal tests of 'significance' of single entries in the periodogram are in general highly subjective, because in many instances spectral features are represented by a cluster of adjacent entries. Renshaw & Ford (1983) adopt a less formal 'censoring approach'. They replace values of $\{I_{pq}\}$ which contribute less than $c$% of total variance (for some $c$ to be determined) by zeros, and $c$ is chosen to be just large enough for most background noise to be removed. The value $c = 400/mn$ % was found appropriate in their work, though it will not be of universal application. To test individual values, entries in the half-spectrum $\{I_{pq}\}$ are first expressed as percentages of the total variance, for they are then approximately distributed as $(100/mn)\chi^2_2$. For example, with $m = n = 32$ critical values for a one-sided test at the 5%, 1% and 0.1% levels are respectively 0.59%, 0.90% and 1.35% of total variance.

Although the addition of noise to the pure cosine wave greatly reduced the contribution of $I_{44}$ to the total variance, at 33.14% it still greatly exceeds the next highest $I_{pq}$-value of 0.69%. In general such dominance is not to be expected, and most $I_{pq}$-elements which exceed the censoring value of $c = 0.4$% (which here number 27) would contribute to the overall shape of the spectral feature. We stress that the censoring approach helps to *identify* possible structure in the periodogram and does *not* constitute a formal *test* procedure.

*The polar spectrum*

The presence of a distinct directional component of pattern, i.e. anisotropy, is amply revealed for both the cosine wave and the cosine wave plus noise by the dominant entries at $I_{44}$. However, the presence of either anisotropy, or just a slight rise over a particular band of frequencies, may not always be visually apparent from the periodogram $\{I_{pq}\}$. Transformation to the corresponding polar spectrum can highlight such features for it represents directional components and scales of pattern separately. Directional components are analyzed through the Θ-spectrum, which is a plot of elements with approximately the same frequency angle $(tan^{-1}(p/q))$. Scales of pattern are analyzed through the $R$-spectrum, which is a plot of elements with approximately the same frequency magnitude $(\sqrt{(p^2 + q^2)})$.

For each value of $I_{pq}$ over the range

$$\begin{array}{lll} p = 0 & ; & q = -n/2, \ldots, -1 \\ p = 1, \ldots, m/2 - 1 & ; & q = -n/2, \ldots, n/2 - 1 \\ p = m/2 & ; & q = -n/2, \ldots, 0 \end{array}$$

we evaluate $r = \sqrt{(p^2 + q^2)}$ and $\theta = tan^{-1}(p/q)$, having first scaled the $I_{pq}$ to ensure that their average value is unity. Next we consider (for example) the groups $0 < r \leqslant 1, 1 < r \leqslant 2, \ldots$ and $-5° < \theta \leqslant 5°$, $5° < \theta \leqslant 15°, \ldots, 165° < \theta \leqslant 175°$ and allocate to each interval the appropriate $I_{pq}$-values. Finally we divide the sum of the $I_{pq}$ in each interval by the number of values counted within it. This yields respectively, the $R$-spectra and Θ-spectra. In the absence of spatial structure all the $R_r$ and $\Theta_\theta$ values have expected value unity. Different periodogram structures may have similar polar representations, and care must be taken in interpretation by referring back to the original sample spectrum. As would be expected, the $R$-spectrum (Fig. 1d) corresponding to the periodogram (Fig. 1c) shows a large peak (at $4\sqrt{2} = 5.66$) in the interval $5 < r \leqslant 6$, whilst the Θ-spectrum (Fig. 1e) has the anticipated maximum (45°) in the interval $35° < \theta \leqslant 45°$. This simple example clearly illustrates how the scale of pattern and wave direction are determined separately from the $R$- and Θ-spectrum, respectively. For the cosine wave with noise both the $R$- and Θ-spectra (Figs. 2d, 2e) have high values considerably in excess of 1 at the same points as for the pattern without noise (Figs. 1d, 1e).

Since the individual $I_{pq}$ are approximately distributed as $(100/mn)\chi^2_2$, then for a particular $R$- or

Θ-interval (say $R_r$ or $\Theta_\theta$) which contains $N$ periodogram elements the polar spectral value for $R_r$ or $\Theta_\theta$ is distributed as $(1/2N)\chi^2_{2N}$. Hence tests of significance at specific $r$- or $\theta$-values can be made. For example the $R$- and Θ-spectra in Figures 2d, 2e have peaks of 11.20 at $r \approx 6$ and 4.57 at $\theta \approx 45°$, respectively. The corresponding polar segments contain 16 and 43 elements, respectively, so the critical values at the 0.1% significance level are $(1/32)\chi^2_{32} = 1.95$ and $(1/86)\chi^2_{86} = 1.54$. Both of these are very small in relation to the computed values (11.20 and 4.57), and so the two polar peaks are extremely significant statistically.

This example illustrates the usefulness of calculating polar spectra because, although a cosine was used as the basis for generating Figure 2a, visually its influence could not be seen in the data.

## Spectra of some simulated patterns

Interpretation of two-dimensional spectra can be assisted by appreciation of the spectra of patterns of known structure, particularly where an observed pattern is thought to be the result of two or more generating processes. Evidence for the influence of

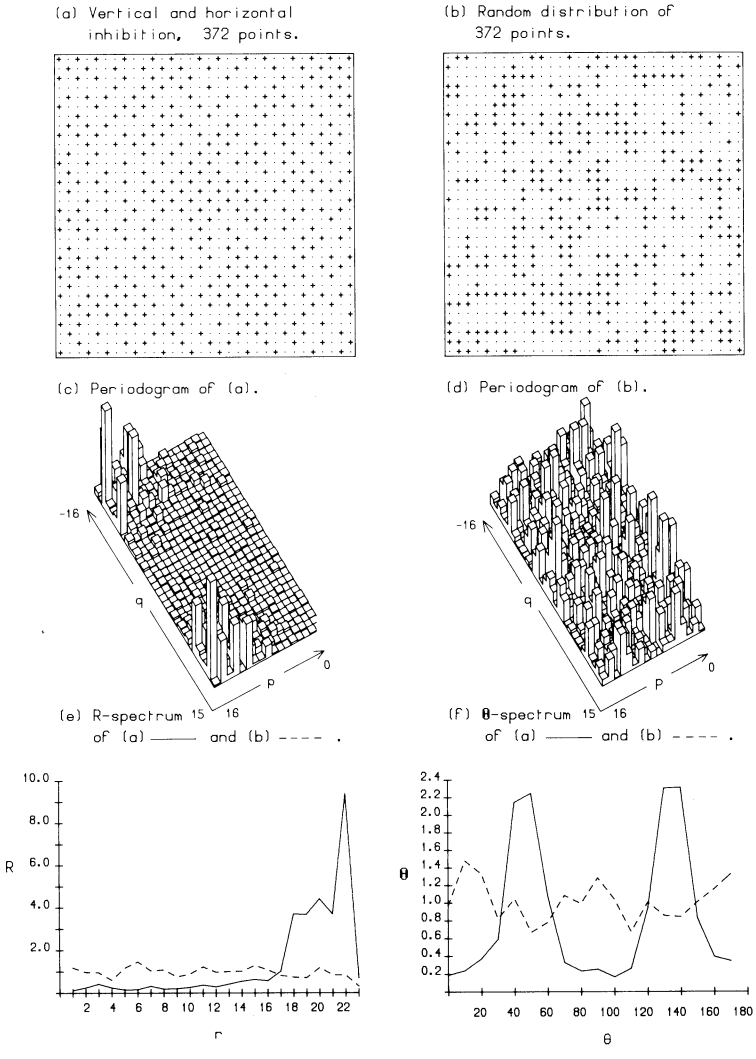


*Fig. 3.* Spatial analysis of two point patterns. (a) simple inhibition process, see text; (b) inhibition-free process for the same number of points, see text; (c) periodogram of (a); (d) periodogram of (b); (e) and (f) $R$- and Θ-spectrum, resp. of (a) and (b).

more than one generating process in a pattern was seen in a Scots pine stand, *Pinus sylvestris* (Renshaw & Ford, 1983) where tree positions were interpreted, not surprisingly in a regularly thinned forest, as showing spatial inhibition whilst the canopy exhibited growth under a directional influence. Here we separately consider the spectra of first an inhibition process and then directional structure. Subsequently (Ford & Renshaw, 1984) we consider their combination in a model for the development of *Epilobium angustifolium* L. communities.

*Inhibition*

A simple inhibition process was simulated (Fig. 3a), the value 1 being placed sequentially at random on a $32 \times 32$ lattice $\{X_{ij}\}$ of 0's, subject to a minimum nearest-neighbour distance of $\sqrt{2}$, until there was no more room for points to be placed (maximum packing). This occurred when 372 of the 1 024 sites were occupied. A minimum separation distance of $\sqrt{2}$ means that adjacent row and column, but not diagonal, sites must be empty, and so there is a strong diagonal structure. In contrast Figure 3b shows a simulated inhibition-free pattern with 372 points placed at random on the lattice but with no site containing more than one point. There are adjacent, non-empty sites on rows and columns as well as on diagonals.

Comparison of the two periodograms (Figs. 3c, 3d) shows that the diagonal inhibition structure features very strongly, with all large periodogram elements being crowded into the SE and SW corners, whilst in contrast the periodogram of the inhibition-free process gives no indication of spectral structure. The respective polar-spectra (Figs. 3e, 3f) confirm these conclusions. The $R$- and $\Theta$-spectra both remain close to 1 for the inhibition-free process, as expected for a random pattern. For the inhibition process the $R$-spectrum peaks at $r =$ 18–22 and the $\Theta$-spectrum peaks at 35°–55° and 125°–145°. These $\theta$-values emphasize the 45° and 135° diagonal structure of the inhibition pattern, and as the diagonal length of the 'sample' area is $32\sqrt{2}$ units the corresponding frequency range of $r$ = 18–22 relates to a scale of pattern in the range $(32\sqrt{2})/22$ to $(32\sqrt{2})/18$ units, i.e. 2.1 to 2.5 units Only with a regular pattern of alternating 0's and 1's could the scale equal 2 exactly.

Generation of both the inhibition and spatially random patterns (Figs. 3a, 3b) involved the use of a random number generator. Further patterns generated by the same processes, but using different random number sequences, yield slightly different periodograms. The range of values in the $R$-spectra generated from 20 independent simulations for both processes are shown in Figure 4. The expected value of the scaled $R$-spectrum for a random distribution is 1 for all values of $r$. The envelope defined by maximum and minimum values from 20 simulations of the random process always encloses 1, and has its least spread at $r = 16$ and its greatest spread at $r = 1$ and $r = 23$ because the low and very high frequency annuli contain few Cartesian values. The envelope from 20 simulations of the inhibition process shows a narrow, slowly increasing band lying well below 1 for $r = 4$ to $r = 14$ after which it increases rapidly, lying above the envelope of the random process for $r = 17$ to 22 with a single exception at $r = 19$. This defines the high frequency pattern of the large number of small, regularly spaced points on the lattice.

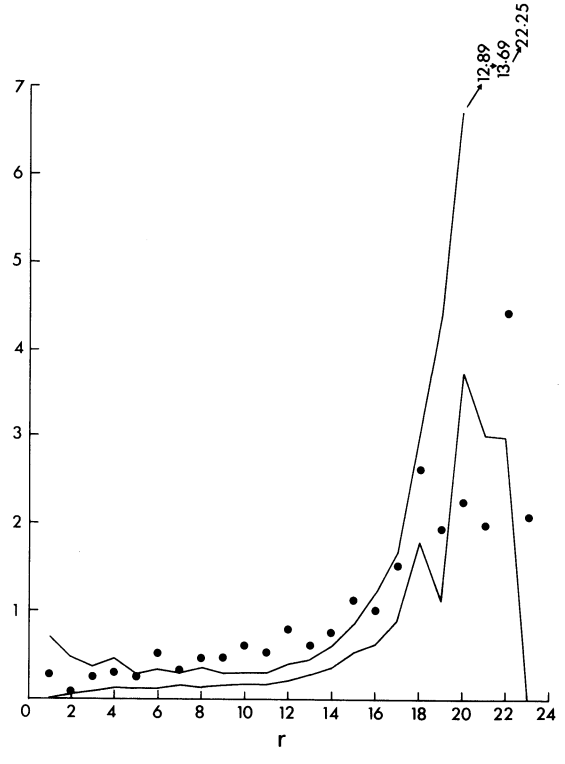


*Fig. 4.* $R$-spectra of patterns generated on a $32 \times 32$ lattice.
—— envelope (max and min values) from 20 simulations, maximum packing with nearest-neighbour distance $\sqrt{2}$;
• one simulation with nearest-neighbour distance $\sqrt{2}$ but 2/3 maximum packing.

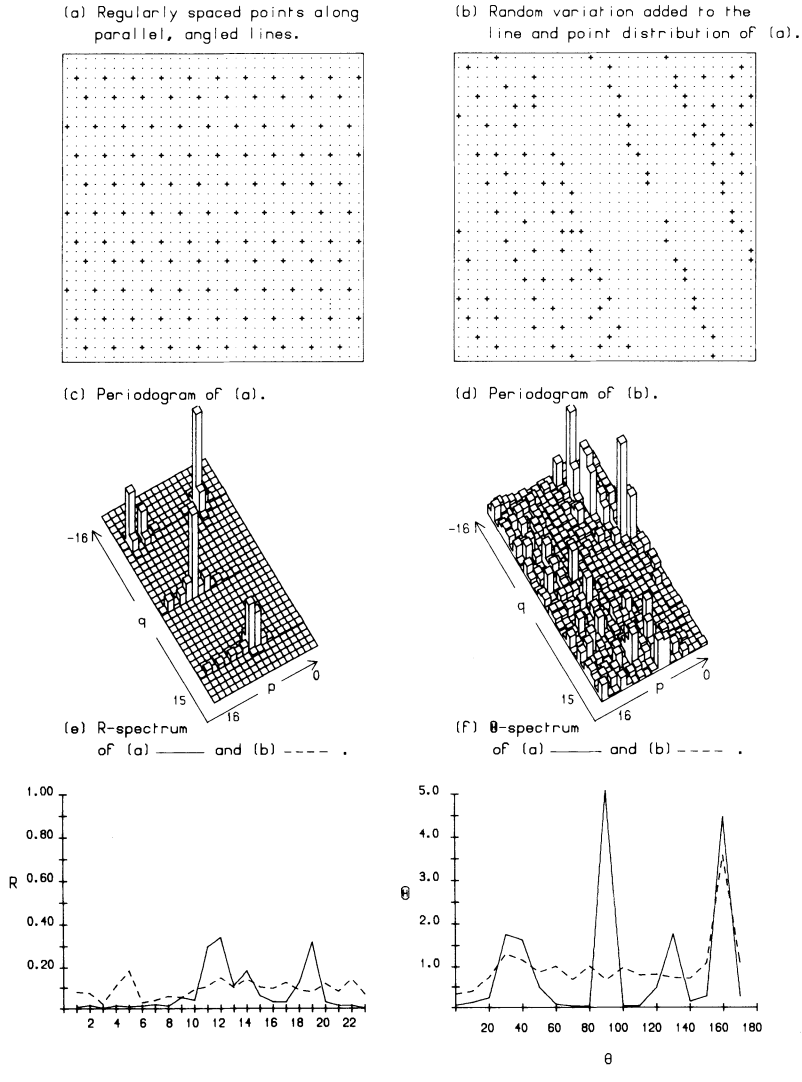


*Fig. 5.* Two models of an invasion process. (a) regularly spaced points along parallel angled lines; (b) random variation added to the line and point distribution of (a), see text; (c) periodogram of (a); (d) periodogram of (b); (e) ($\times 10^{-1}$) and (f) $R$- and $\Theta$-spectrum, resp. of (a) and (b).

The detection of an inhibition process depends on packing density. We found that as the number of occupied sites in the inhibition process were reduced to 2/3 of maximum packing the intensity of spectral entries dropped (Fig. 4) though the overall shape remained. At maximum packing the inhibition pattern is strongly diagonal (Fig. 3a), being the result of simulating the process on a square grid. The inhibition distance is $\sqrt{2}$ and 96.2% of nearest-neighbour distances are at $\sqrt{2}$ units, 2.2% at 2, and 1.6% at $\sqrt{5}$ units, which yields a high contribution from frequencies above 16 on the 45° and 135° diagonals.

As the number of occupied sites in an inhibition process is increased then the annulus of significant entries in the Cartesian spectrum is moved to higher frequencies. The lowest frequency approximates the maximum, and the highest the minimum, nearest-neighbour distances. This structure can be seen in the analyses of both the distribution of plants of willow herb (Ford & Renshaw, 1984) and the spacing of individual trees at Thetford Forest analyzed by Renshaw & Ford (1983, their Fig. 6b).

*Spread in a preferred direction*

Invasion of an area by a plant species may be directional and the resulting spatial pattern therefore anisotropic. Many plants spread by horizontal roots, rhizomes, or similar structures creeping underground, which produce aerial shoots at intervals. Some problems in detecting the directional component of an underlying pattern, for example a spreading root system, from the distribution of units on it, for example plants, were examined with simulations of a simple model. Points of origin of roots were placed a constant distance ($d$) apart along a base line, and the angle of spread ($\theta$) from it was distributed as $N(\mu_\theta, \sigma_\theta^2)$, i.e. as a Normal random variable with mean $\mu_\theta$ and variance $\sigma_\theta^2$. Aerial shoots were positioned sequentially along each root a distance $m$ apart where $m$ was distributed as $N(\mu_m, \sigma_m^2)$. Grid counts on a $32 \times 32$ matrix were made of the presence of aerial shoots over an area distant from the base line (to eliminate the regularity of start positions) for various combinations of the parameters $d$, $\mu_\theta$, $\sigma_\theta^2$, $\mu_m$ and $\sigma_m^2$.

The values $\mu_\theta = 70°$ and $\mu_m = d = 3$ were retained throughout. With $\sigma_\theta^2 = \sigma_m^2 = 0$ (Fig. 5a) the process is deterministic and the largest single spectral entry was 14.4% at (4, -11). The corresponding $\theta$-angle is 160° which is the direction *across* the roots, and so *their* corresponding direction is at right angles, i.e. 160°-90° = 70° (Fig. 5f). However, the extreme *regularity* of the pattern, i.e. parallel lines of equidistant points, was such that additional regularity exists in the data, notably along diagonals to the generated lines, and this additional structure was apparent in the spectrum: (i) 22.8% centered at (11,0) - the result of 1's in every third (sometimes second) row; (ii) 16.8% centered at (15, -11) - conjugate waves angled around $\mu_\theta = 36°$; and, (iii) 20.8% centered at (8, 11) - conjugate waves angled around $\mu_\theta = 126°$. Similar conjugate patterns have been demonstrated in other *regular* patterns (Table IV and Fig. 13 in Ford, 1976), and failure to appreciate them can lead to wrong interpretation.

Retaining the parallel line structure by keeping $\sigma_\theta^2 = 0$ but marginally increasing $\sigma_m^2$ greatly reduced these conjugate patterns, and their associated spectra were downgraded to a low-intensity band running from features (ii) to (i) to (iii). When we also allowed $\sigma_\theta^2 > 0$ (in Fig. 5b, $\sigma_\theta^2 = 4.0$) the simulated patterns consisted of lines in various orientations, and although the Cartesian (4, -11) value (Fig. 5d) was diffused amongst its neighbours the polar $\Theta$-spectrum still provided a good detector for anisotropy (Fig. 5f). For example, values for root direction in two typical simulations with: (i) $\sigma_m^2 = 0.25$, $\sigma_\theta^2 = 4.0$ were 0.63 at 60°, 3.72 at 70°, 1.14 at 80° and 0.44 at 90°; (ii) $\sigma_m^2 = 1.0$, $\sigma_\theta^2 = 400.0$ were 0.89 at 60°, 1.72 at 70°, 1.67 at 80° and 0.69 at 90°. In case (ii) the orientation of the simulated roots varied considerably, as did the distance between shoots on the same root, yet the general direction of invasion was still easily discerned from the $\Theta$-spectrum. Thus even if an ecological data set contains a very weak directional component then it is likely that the $\Theta$-spectrum will detect it.

## Discussion

Two-dimensional spectral analysis as we present it here uses four functions which combine to highlight different aspects of pattern structure. This, in combination with the censoring approach used to assess the significance of spectral entries, makes it a powerful technique. It is particularly suited to the general interrogation of data for the occurrence of pattern, and is limited only by the requirements that the pattern comprises features which are repeated within the sample frame and are no smaller in scale than twice the distance between the points of the sample grid.

It may appear that two-dimensional analysis can reveal features which would not be expected from the pattern-generating mechanism, as in the 'conjugate wave' example above. This is not the case, for simple generating rules can produce complex patterns and one must be aware of this in interpretation. However, as we demonstrate in Figure 5, addition of variability to the generating process disrupts such second-order features, and in analyzing data from the natural environment we have not found the occurrence of conjugate patterns a problem.

To perform a two-dimensional spectral analysis data must first be collected in a contiguous two-dimensional array. However, discussions on methodology, notably Hill (1973) and Usher (1975), have concentrated on pattern analysis of one-dimensional arrays. Two points must be made. First, providing the intensity of sampling is correct we have repeatedly found that spectral analysis of only

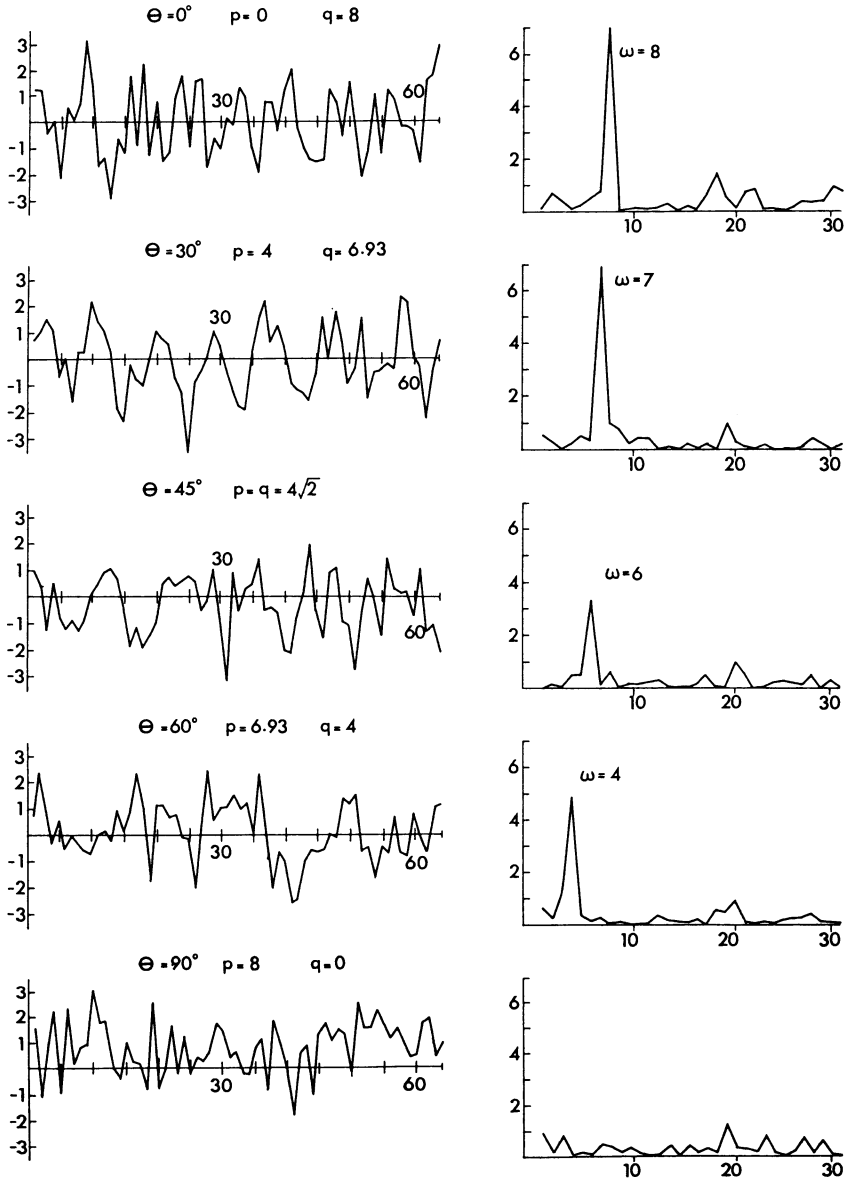


*Fig. 6.* A series of one-dimensional transects taken at various angles ($\theta$) through a two-dimensional cosine wave with added noise, and their respective periodograms. $\theta$ is the angle between the transect and the direction of travel of the wave. $\omega$ is the frequency of pattern repeats along the transect. $p$ and $q$ are the frequencies of pattern repeats along each axis, with $\sqrt{(p^2 + q^2)} = 8$.

a $32 \times 32$ array of sample points gives an adequate analysis. Second, analysis of one-dimensional arrays *assumes* that there is no directional component in the pattern, i.e. that it is isotropic. The effect of sampling a cosine wave of wavelength 8 with added noise by a series of one-dimensional transects at different angles to the direction of the cosine wave illustrates this problem. When a transect of 64 points was taken along the direction of travel of the wave then there was a dominant entry in the spectrum at the expected frequency $\omega = 64/8 = 8$ (Fig. 6). However, as the transect was made at increasing angles to the direction of travel of the wave the dominant entry appeared at lower frequencies. For an angle of 30° $\omega = 7$, for 45° $\omega = 6$, for 60° $\omega = 4$, and when the transect runs at 90° to the wave direction then no spectral features are apparent as the data are pure noise.

Thus although a linear transect may detect the *presence* of pattern, when the direction of the wave is unknown the one-dimensional analysis cannot determine the *scale* of pattern. From the analysis of ecological data we have found directional components to be widespread and consider the general *a priori* assumption of isotropy to be unacceptable.

Two-dimensional spectral analysis has the further advantage over one-dimensional analysis that in general more periodogram values are contained in the spectral features. This means that further smoothing is usually unnecessary which is rarely so for one-dimensional spectra. Moreover, as the *R*- and Θ-spectra are an average of periodogram values their smoothness is ensured.

## References

Ford, E. D., 1976. The canopy of a Scots pine forest: description of a surface of complex roughness. Agric. Met. 17: 9–32.

Ford, E. D. & Renshaw, E., 1984. The interpretation of process from pattern using two-dimensional spectral analysis: single species patterns in vegetation. Vegetatio 56: 113–123.

Greig-Smith, P. J., 1952. The use of random and contiguous quadrats in the study of the structure of plant communities. Ann. Bot. 16: 293–316.

Greig-Smith, P. J., 1979. Pattern in vegetation. J. Ecol. 67: 755–799.

Hill, M. O., 1973. The intensity of spatial pattern in plant communities. J. Ecol. 61: 225–235.

Renshaw, E. & Ford, E. D., 1983. The interpretation of process from pattern using two-dimensional spectral analysis: methods and problems of interpretation. Appl. Statist. 32: 51–63.

Ripley, B. D., 1978. Spectral analysis and the analysis of pattern in plant communities. J. Ecol. 66: 965–981.

Usher, M. B., 1975. Analysis of pattern in real and artificial plant populations. J. Ecol. 63: 569–586.

Watt, A. S., 1947. Pattern and process in the plant community. J. Ecol. 35: 1–22.

Accepted 22.11.1983.